

THÈSE DE DOCTORAT
DE SORBONNE UNIVERSITÉ

Spécialité : Physique

École doctorale n°564: Physique en Île-de-France

réalisée

au Laboratoire Kastler Brossel

sous la direction de Pierre-François Cohadon

présentée par

Pierre-Edouard Jacquet

pour obtenir le grade de :

DOCTEUR DE SORBONNE UNIVERSITÉ

Sujet de la thèse :

Progress towards cryogenic squeezed light optomechanics

soutenue le ?? ??? 2025

devant le jury composé de :

M.	Mr.	Rapporteur
M.	Mr.	Rapporteur
M.	Mr.	Examineur
Mme.	coucou	Examinatrice
Mme.	salut	Présidente du Jury
M.	aurevoir	Directeur de thèse

Contents

I	Introduction	1
I.1	Historical background	1
I.2	State of the art	1
I.3	Relevance of this work	1
II	Theory: background	3
II.1	Quantum Optics Concepts	3
II.1.1	Quantum Description of Light	3
II.1.2	Optical Field Modulations	8
II.1.3	Quantum Noise and Uncertainty	9
II.1.4	Sideband Representation	9
II.2	Optical Cavities : Basics	9
II.2.1	Cavity types and Resonance Conditions	9
II.2.2	Spatial and Longitudinal Modes	9
II.2.3	Static and Dynamical effects	9
II.3	Optical Cavities : Three Mirror Cavities	9
II.3.1	9
II.4	Cavity Optomechanics	9
II.4.1	Radiation Pressure Coupling	9
II.4.2	Quantum Langevin Equations	9
II.4.3	Mechanical Resonators	9
II.4.4	Noise spectra	9
II.4.5	Three Mirror Cavities as Novel Optomechanical Systems	9
II.5	Squeezed Light Theory	9
II.5.1	Single-mode Squeezing	9
II.5.2	Noise Spectra	9
II.5.3	Frequency-dependent Squeezing and its use	9
II.6	Numerical Simulations of FDS Optomechanical Experiments	10
III	Experimental Methods	11
III.1	Generation of Squeezed Light	11
III.1.1	Bowtie-type Optical Parametric Oscillator (OPO)	11
III.1.2	Phase Matching and Nonlinear Crystals	11
III.1.3	Filter Cavities for Squeezing Rotation	11

III.2 Optical Locking Techniques	11
III.2.1 Michelson-type locking	11
III.2.2 Pound-Drever-Hall Locking	11
III.2.3 Phase-Locked Loops	11
III.2.4 FPGA and PYRPL Control Implementation	11
III.3 Quadrature Measurement Techniques	11
III.3.1 Direct Detection with Photodiodes	11
III.3.2 Balanced Homodyne Detection	11
III.3.3 Local Oscillator Design and Control	11
IV Experiments : Optomechanical Three-Mirror Cavity Systems (MATE)	13
IV.1 System Description and Setup	13
IV.1.1 Cavity Geometry and CAD Models	13
IV.1.2 Laser Source and Optical Layout	13
IV.1.3 Alignment Procedures	13
IV.2 Middle Mirror as Mechanical Resonator	13
IV.2.1 Plane Membranes: Design and Characterization	13
IV.2.2 Phononic Crystals: Dahlia Pattern	13
IV.2.3 Fabrication and Performance Metrics	13
IV.3 Experimental Characterization	13
IV.3.1 Cavity Mode Scanning and Modematching	13
IV.3.2 Locking Techniques and Stability	13
IV.3.3 Ringdown Measurements and Q-factor Analysis	13
IV.4 Data Acquisition and Analysis	14
IV.4.1 Measurement Setup and Instrumentation	14
IV.4.2 Spectral Acquisition and Processing	14
IV.4.3 Feedback Control Implementation	14
IV.5 Design of an Optomechanical Fibered Cavity	14
IV.5.1 Design considerations	14
V Experiments: Frequency Dependent Squeezing	15
V.1 OPO Resonance and Locking	15
V.1.1 Resonance Conditions and Sweeps	15
V.1.2 Lock Acquisition and Optimization	15
V.1.3 Stability Characterization	15
V.2 Quadrature Spectral Analysis	15
V.2.1 Detection of Squeezing and Anti-squeezing	15
V.2.2 Spectral Variation with Frequency	15
V.2.3 Optimal Quadrature Conditions	15
V.3 Filter Cavity Concept	15
V.3.1 Virgo Filter Cavity	15
V.3.2 Thermal effects in bichromatic locks	15
A Un appendice	19

Chapter I

Introduction

- I.1 Historical background**
- I.2 State of the art**
- I.3 Relevance of this work**

Chapter II

Theory: background

This chapter will cover the elementary concepts required to describe an membrane based optomechanical system in a quantum regime. We will first recall basics on optical field quantization as well describing coherent and squeezed light field, to then turn to the more specific frequency dependent squeezed light field. Secondly, we will cover the mathematical description of a mechanical resonator interacting with a generic coherent optical field, highlighting the differences with the seminal optomechanical system of a mirror on a spring. Finally, we will derive the equations of motions of a membrane based optomechanical system with frequency dependent squeezed optical fields.

II.1 Quantum Optics Concepts

II.1.1 Quantum Description of Light

We introduce briefly field quantization concepts needed to describe monochromatic field propagation and measurements. key words : eigenmodes of the field, quantization, annihilation operators, quadratures, phase space, displacement operators, squeezing operators, coherent states, generic squeezed states,

Quantised Electromagnetic Field

We consider the quantised electromagnetic field in volume V . The electric field operator can be expressed in the Heisenberg picture as:

$$\hat{\mathbf{E}}(\mathbf{r}, t) = i \sum_{\ell} \mathcal{E}_{\ell} \left[\hat{a}_{\ell} \mathbf{f}_{\ell}(\mathbf{r}) e^{-i\omega_{\ell} t} - \hat{a}_{\ell}^{\dagger} \mathbf{f}_{\ell}^*(\mathbf{r}) e^{i\omega_{\ell} t} \right] \quad (\text{II.1})$$

where $\mathcal{E}_{\ell} = \sqrt{\frac{\hbar\omega_{\ell}}{2\varepsilon_0 V}}$ is the field per photon in mode ℓ with \hbar the reduced Planck constant, ω_{ℓ} the angular frequency of mode ℓ and ε_0 the vacuum permittivity, $\mathbf{f}_{\ell}(\mathbf{r})$ are spatial mode functions satisfying orthonormality, and $(\hat{a}_{\ell}, \hat{a}_{\ell}^{\dagger})$ are the time dependent annihilation and creation operators associated with each mode ℓ satisfying the canonical commutation relations

$$[\hat{a}_{\ell}, \hat{a}_{\ell'}^{\dagger}] = \delta_{\ell\ell'}, \quad [\hat{a}_{\ell}, \hat{a}_{\ell'}] = 0, \quad [\hat{a}_{\ell}^{\dagger}, \hat{a}_{\ell'}^{\dagger}] = 0$$

Fock states

In this description of the optical field, each mode ℓ is modeled as a quantum harmonic oscillator with a discrete set of energy eigenstates known as *Fock states* or number states, denoted $|n_\ell\rangle$. These states form an orthonormal basis and satisfy $\hat{n}_\ell |n_\ell\rangle = n_\ell |n_\ell\rangle$, where \hat{n}_ℓ is the number operator defined by

$$\hat{n}_\ell = \hat{a}_\ell^\dagger \hat{a}_\ell.$$

The action of the creation and annihilation operators on these states is given by

$$\hat{a}_\ell |n_\ell\rangle = \sqrt{n_\ell} |n_\ell - 1\rangle, \quad \hat{a}_\ell^\dagger |n_\ell\rangle = \sqrt{n_\ell + 1} |n_\ell + 1\rangle.$$

They allow transitions between Fock states by lowering or raising the photon number in mode ℓ by one unit. The vacuum state $|0_\ell\rangle$ is annihilated by \hat{a}_ℓ , satisfying $\hat{a}_\ell |0_\ell\rangle = 0$. Thus, the Hamiltonian for the electromagnetic field becomes a sum of harmonic oscillator energies:

$$\hat{H} = \sum_\ell \hbar\omega_\ell \left(\hat{n}_\ell + \frac{1}{2} \right) \quad (\text{II.2})$$

Quasi monochromatic fields

In realistic optical systems such as lasers, the electromagnetic field is rarely perfectly monochromatic. Instead, it exhibits a finite spectral linewidth due to spontaneous emission, phase noise, or intentional modulation. These effects cause the amplitude and phase of the optical field to evolve slowly compared to the optical frequency ω_ℓ .

As a result, the complex amplitude associated with each mode, typically captured by the Heisenberg-picture annihilation operator $\hat{a}_\ell(t)$, acquires an explicit time dependence beyond the standard fast-oscillating term $e^{-i\omega_\ell t}$. This slow temporal variation reflects the underlying physics: for instance, amplitude or phase modulation, feedback-induced dynamics, or noise processes can all modulate the quantum state in time. Consequently, in the quasi-monochromatic regime, one often separates the field into a rapidly oscillating carrier and a slowly varying envelope encoded in $\hat{a}_\ell(t)$, allowing a spectrally resolved yet temporally adaptive description of the field.

Linearization of the optical field: mean field and fluctuations

We often consider a single spatial mode of the electromagnetic field with optical frequency ω_0 , and assume the presence of a strong coherent field. In this regime, the annihilation operator is decomposed as $\hat{a}(t) = \bar{\alpha}(t) + \delta\hat{a}(t)$, where $\bar{\alpha}(t)$ is a classical complex amplitude and $\delta\hat{a}(t)$ represents quantum fluctuations. Linearizing the electric field operator then yields:

$$\hat{\mathbf{E}}(\mathbf{r}, t) = i\mathcal{E} \left[\bar{\alpha}(t)\mathbf{f}(\mathbf{r})e^{-i\omega_0 t} - \bar{\alpha}^*(t)\mathbf{f}^*(\mathbf{r})e^{i\omega_0 t} \right] + i\mathcal{E} \left[\delta\hat{a}(t)\mathbf{f}(\mathbf{r})e^{-i\omega_0 t} - \delta\hat{a}^\dagger(t)\mathbf{f}^*(\mathbf{r})e^{i\omega_0 t} \right] \quad (\text{II.3})$$

The first line represents the full electric field operator, while the second separates it into a classical component, involving the coherent amplitude $\bar{\alpha}(t)$, and a quantum fluctuation term $\delta\hat{a}(t)$. This linearization simplifies the analysis of the field, allowing us to treat the coherent part as a classical field and the fluctuations as a quantum harmonic oscillator. The field Hamiltonian then reduces to a single-mode harmonic oscillator form:

$$\hat{H} = \hbar\omega_0 \left(\delta\hat{a}^\dagger \delta\hat{a} + \frac{1}{2} \right), \quad (\text{II.4})$$

where $\delta\hat{a}$ is the annihilation operator for the fluctuations. The coherent part contributes a constant energy offset, while the fluctuations behave as a quantum harmonic oscillator with frequency ω_0 . This Hamiltonian now features an explicit time dependence through the coherent amplitude $\bar{\alpha}(t)$, which can vary slowly compared to the optical frequency. Importantly, the fluctuation operators retain the canonical bosonic commutation relations:

$$[\delta\hat{a}(t), \delta\hat{a}^\dagger(t)] = 1, \quad [\delta\hat{a}(t), \delta\hat{a}(t)] = 0, \quad [\delta\hat{a}^\dagger(t), \delta\hat{a}^\dagger(t)] = 0.$$

These ensure that the quantized nature of the field is preserved under linearization, with $\delta\hat{a}(t)$ and $\delta\hat{a}^\dagger(t)$ obeying the same algebra as the original field operators.

Remarks:

- The linearization procedure is valid when the coherent amplitude $\bar{\alpha}(t)$ is much larger than the quantum fluctuations, i.e., $|\bar{\alpha}(t)| \gg \langle \delta\hat{a}^\dagger \delta\hat{a} \rangle^{1/2}$.
- This approach is widely used in quantum optics and optomechanics to simplify the analysis of systems driven by strong classical fields, such as lasers.
- The separation into mean field and fluctuations allows us to treat the quantum noise properties independently from the classical dynamics.
- The quantum fluctuation operators $\delta\hat{a}(t)$ describe vacuum or squeezed noise, and their statistics determine the ultimate sensitivity limits in measurement schemes.
- Linearization is the starting point for deriving quantum Langevin equations and for analyzing noise spectra in optomechanical systems.

Quadrature Operators

To describe the phase space properties of a field mode, we define the Hermitian quadrature operators $\hat{a}_{1,l}$ and $\hat{a}_{2,l}$ as

$$\begin{aligned} \hat{a}_{1,l} &= \hat{a}_\ell + \hat{a}_\ell^\dagger \\ \hat{a}_{2,l} &= \hat{a}_\ell - \hat{a}_\ell^\dagger \end{aligned} \quad (\text{II.5})$$

More generally we can define arbitrary quadrature operators as

$$\begin{aligned} \hat{a}_{\theta,l} &= e^{i\theta} \hat{a}_\ell + e^{-i\theta} \hat{a}_\ell^\dagger \\ &= \cos \theta \hat{a}_{1,l} + \sin \theta \hat{a}_{2,l} \end{aligned} \quad (\text{II.6})$$

where we notice that $\hat{a}_{1,l} = \hat{a}_{\theta=0,l}$ and $\hat{a}_{1,l} = \hat{a}_{\theta=\pi/2,l}$. These are Hermitian operators corresponding to measurable observables and satisfy the commutation relation

$$[\hat{a}_{\theta,l}, \hat{a}_{\theta+\pi/2,l}] = 2i \quad (\text{II.7})$$

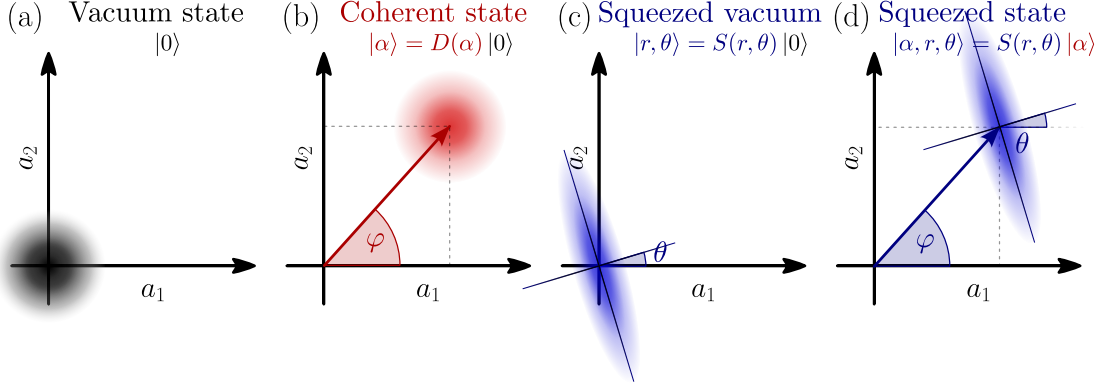


Fig. II.1 Phase-space representations of quantum states and transformations. (a) Wigner function of the vacuum state: a circular Gaussian centered at the origin, representing equal quantum fluctuations in both quadratures X_1 and X_2 . (b) Wigner function of a coherent state: a displaced circular Gaussian, showing a shift in phase space along an angle φ with unchanged, isotropic noise. (c) Wigner function of a squeezed vacuum state: an elliptical Gaussian centered at the origin, with reduced noise along a rotated quadrature X_θ and increased noise in the orthogonal direction. (d) Wigner function of a displaced squeezed state: an ellipse shifted away from the origin, combining anisotropic fluctuations and a nonzero mean amplitude. The displacement angle φ and squeezing angle θ are independent.

Uncertainty Principle and Quantum Noise

For two generic Hermitian operators \hat{A} and \hat{B} , the Heisenberg uncertainty principle reads as

$$\Delta\hat{A}\Delta\hat{B} \geq \frac{1}{2}|\langle[\hat{A}, \hat{B}]\rangle| \quad (\text{II.8})$$

where we defines $\Delta\hat{A} = \sqrt{|\langle\hat{A}^2\rangle - \langle\hat{A}\rangle^2|}$. This defines the minimum amount of quantum noise (vacuum fluctuations) in the electromagnetic field. Applying this equation to the quadratures defined above we get

$$\begin{aligned} \Delta\hat{a}_{1,l}\Delta\hat{a}_{2,l} &\geq 1 \\ \Delta\hat{a}_{\theta,l}\Delta\hat{a}_{\theta+\pi/2,l} &\geq 1 \end{aligned} \quad (\text{II.9})$$

Coherent States

Coherent states $|\alpha_{\omega,\ell}\rangle$ are eigenstates of the annihilation operator:

$$\hat{a}_{\omega,\ell}|\alpha_{\omega,\ell}\rangle = \alpha_{\omega,\ell}|\alpha_{\omega,\ell}\rangle \quad (\text{II.10})$$

They can be generated by displacing the vacuum:

$$|\alpha_{\omega,\ell}\rangle = \hat{D}(\alpha_{\omega,\ell})|0\rangle, \quad \hat{D}(\alpha) = \exp(\alpha\hat{a}^\dagger - \alpha^*\hat{a}) \quad (\text{II.11})$$

They exhibit:

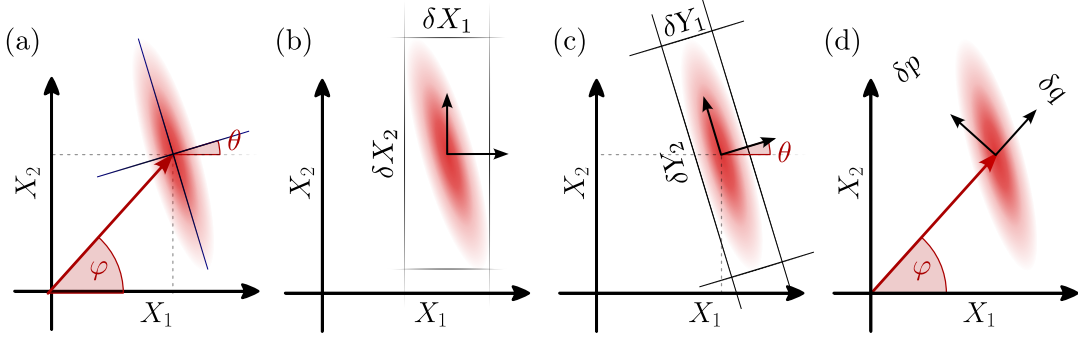


Fig. II.2 Phase-space representations of quantum states and transformations. (a) Wigner function of the vacuum state: a circular Gaussian centered at the origin, representing equal quantum fluctuations in both quadratures X_1 and X_2 . (b) Wigner function of a coherent state: a displaced circular Gaussian, showing a shift in phase space along an angle φ with unchanged, isotropic noise. (c) Wigner function of a squeezed vacuum state: an elliptical Gaussian centered at the origin, with reduced noise along a rotated quadrature X_θ and increased noise in the orthogonal direction. (d) Wigner function of a displaced squeezed state: an ellipse shifted away from the origin, combining anisotropic fluctuations and a nonzero mean amplitude. The displacement angle φ and squeezing angle θ are independent.

- Minimum uncertainty: $\Delta q = \Delta p = 1/\sqrt{2}$
- Classical-like dynamics
- Poissonian photon statistics

Squeezed States

Squeezed states reduce the variance of one quadrature below vacuum level:

$$|\xi_{\omega,\ell}\rangle = \hat{S}(\xi_{\omega,\ell})|0\rangle \quad (\text{II.12})$$

$$\hat{S}(\xi) = \exp \left[\frac{1}{2} (\xi^* \hat{a}^2 - \xi \hat{a}^{\dagger 2}) \right], \quad \xi = r e^{i\phi} \quad (\text{II.13})$$

For phase quadrature squeezing ($\phi = 0$):

$$\Delta q_{\omega,\ell} = e^{-r}/\sqrt{2}, \quad \Delta p_{\omega,\ell} = e^r/\sqrt{2} \quad (\text{II.14})$$

Squeezed light is a key resource for precision metrology and quantum information.

This concludes our introduction to the quantum description of light, setting the stage for modelling interactions between quantum optical fields and mechanical resonators.

II.1.2 Optical Field Modulations

Linearization of the Electric Field and Modulation Sidebands

We consider a single optical mode with a strong coherent drive. The annihilation operator is linearized as:

$$\hat{a}(t) \rightarrow \bar{\alpha}(t) + \delta\hat{a}(t) \quad (\text{II.15})$$

where $\bar{\alpha}(t) \in \mathbb{C}$ is the classical coherent amplitude and $\delta\hat{a}(t)$ captures quantum fluctuations.

The classical part of the electric field is then:

$$\mathbf{E}_{\text{cl}}(\mathbf{r}, t) = i\sqrt{\frac{\hbar\omega}{2\varepsilon_0}} \left[\mathbf{f}(\mathbf{r}) \bar{\alpha}(t) e^{-i\omega t} - \mathbf{f}^*(\mathbf{r}) \bar{\alpha}^*(t) e^{i\omega t} \right] \quad (\text{II.16})$$

We now consider two types of sinusoidal modulation at frequency Ω :

Amplitude Modulation (AM)

Let the coherent amplitude be modulated in amplitude:

$$\bar{\alpha}(t) = \bar{\alpha}_0 (1 + \epsilon_a \cos(\Omega t)) = \bar{\alpha}_0 \left(1 + \frac{\epsilon_a}{2} e^{i\Omega t} + \frac{\epsilon_a}{2} e^{-i\Omega t} \right) \quad (\text{II.17})$$

with $\epsilon_a \ll 1$. The conjugate is:

$$\bar{\alpha}^*(t) = \bar{\alpha}_0^* \left(1 + \frac{\epsilon_a}{2} e^{i\Omega t} + \frac{\epsilon_a}{2} e^{-i\Omega t} \right) \quad (\text{II.18})$$

Substituting into the field expression:

$$\begin{aligned} \mathbf{E}_{\text{cl}}^{(\text{AM})}(\mathbf{r}, t) = i\sqrt{\frac{\hbar\omega}{2\varepsilon_0}} & \left[\mathbf{f}(\mathbf{r}) \bar{\alpha}_0 \left(e^{-i\omega t} + \frac{\epsilon_a}{2} e^{-i(\omega-\Omega)t} + \frac{\epsilon_a}{2} e^{-i(\omega+\Omega)t} \right) \right. \\ & \left. - \mathbf{f}^*(\mathbf{r}) \bar{\alpha}_0^* \left(e^{i\omega t} + \frac{\epsilon_a}{2} e^{i(\omega-\Omega)t} + \frac{\epsilon_a}{2} e^{i(\omega+\Omega)t} \right) \right] \end{aligned} \quad (\text{II.19})$$

Phase Modulation (PM)

Now consider phase modulation of the coherent amplitude:

$$\bar{\alpha}(t) = \bar{\alpha}_0 e^{i\epsilon_\phi \cos(\Omega t)} \approx \bar{\alpha}_0 (1 + i\epsilon_\phi \cos(\Omega t)) = \bar{\alpha}_0 \left(1 + \frac{i\epsilon_\phi}{2} e^{i\Omega t} + \frac{i\epsilon_\phi}{2} e^{-i\Omega t} \right) \quad (\text{II.20})$$

and

$$\bar{\alpha}^*(t) \approx \bar{\alpha}_0^* \left(1 - \frac{i\epsilon_\phi}{2} e^{i\Omega t} - \frac{i\epsilon_\phi}{2} e^{-i\Omega t} \right) \quad (\text{II.21})$$

Substituting into the field:

$$\begin{aligned} \mathbf{E}_{\text{cl}}^{(\text{PM})}(\mathbf{r}, t) = i\sqrt{\frac{\hbar\omega}{2\varepsilon_0}} & \left[\mathbf{f}(\mathbf{r}) \bar{\alpha}_0 \left(e^{-i\omega t} + \frac{i\epsilon_\phi}{2} e^{-i(\omega-\Omega)t} + \frac{i\epsilon_\phi}{2} e^{-i(\omega+\Omega)t} \right) \right. \\ & \left. - \mathbf{f}^*(\mathbf{r}) \bar{\alpha}_0^* \left(e^{i\omega t} - \frac{i\epsilon_\phi}{2} e^{i(\omega-\Omega)t} - \frac{i\epsilon_\phi}{2} e^{i(\omega+\Omega)t} \right) \right] \end{aligned} \quad (\text{II.22})$$

Interpretation

In both cases, the field contains a carrier at frequency ω and two sidebands at $\omega \pm \Omega$. Amplitude modulation results in sidebands that are in phase with the carrier, while phase modulation produces sidebands with a $\pm\pi/2$ phase shift relative to the carrier.

II.1.3 Quantum Noise and Uncertainty**II.1.4 Sideband Representation****II.2 Optical Cavities : Basics****II.2.1 Cavity types and Resonance Conditions****II.2.2 Spatial and Longitudinal Modes****II.2.3 Static and Dynamical effects****II.3 Optical Cavities : Three Mirror Cavities****II.3.1****II.4 Cavity Optomechanics****II.4.1 Radiation Pressure Coupling****II.4.2 Quantum Langevin Equations****II.4.3 Mechanical Resonators****II.4.4 Noise spectra****II.4.5 Three Mirror Cavities as Novel Optomechanical Systems****II.5 Squeezed Light Theory****II.5.1 Single-mode Squeezing****II.5.2 Noise Spectra****II.5.3 Frequency-dependent Squeezing and its use**

II.6 Numerical Simulations of FDS Optomechanical Experiments

lets write smth here

Chapter III

Experimental Methods

III.1 Generation of Squeezed Light

- III.1.1 Bowtie-type Optical Parametric Oscillator (OPO)
- III.1.2 Phase Matching and Nonlinear Crystals
- III.1.3 Filter Cavities for Squeezing Rotation

III.2 Optical Locking Techniques

- III.2.1 **Michelson-type locking**
- III.2.2 Pound-Drever-Hall Locking
- III.2.3 Phase-Locked Loops
- III.2.4 FPGA and PYRPL Control Implementation

III.3 Quadrature Measurement Techniques

- III.3.1 Direct Detection with Photodiodes
- III.3.2 Balanced Homodyne Detection
- III.3.3 Local Oscillator Design and Control

Chapter IV

Experiments : Optomechanical Three-Mirror Cavity Systems (MATE)

IV.1 System Description and Setup

IV.1.1 Cavity Geometry and CAD Models

IV.1.2 Laser Source and Optical Layout

IV.1.3 Alignment Procedures

IV.2 Middle Mirror as Mechanical Resonator

IV.2.1 Plane Membranes: Design and Characterization

IV.2.2 Phononic Crystals: Dahlia Pattern

IV.2.3 Fabrication and Performance Metrics

IV.3 Experimental Characterization

IV.3.1 Cavity Mode Scanning and Modematching

IV.3.2 Locking Techniques and Stability

IV.3.3 Ringdown Measurements and Q-factor Analysis

IV.4 Data Acquisition and Analysis

IV.4.1 Measurement Setup and Instrumentation

IV.4.2 Spectral Acquisition and Processing

IV.4.3 Feedback Control Implementation

IV.5 Design of an Optomechanical Fibered Cavity

IV.5.1 Design considerations

Chapter V

Experiments: Frequency Dependent Squeezing

V.1 OPO Resonance and Locking

- V.1.1 Resonance Conditions and Sweeps**
- V.1.2 Lock Acquisition and Optimization**
- V.1.3 Stability Characterization**

V.2 Quadrature Spectral Analysis

- V.2.1 Detection of Squeezing and Anti-squeezing**
- V.2.2 Spectral Variation with Frequency**
- V.2.3 Optimal Quadrature Conditions**

V.3 Filter Cavity Concept

- V.3.1 Virgo Filter Cavity**
- V.3.2 Thermal effects in bichromatic locks**

Summary, conclusion and perspectives

Appendix A

Un appendice

I'll write something here.

Sujet : Progress towards cryogenic squeezed light optomechanics

Résumé : .

Mots clés : Optomecanique, Lumière comprimée, Cavit  de grande Finesse, Interferom trie, Bruit thermique, Bruit de grenaille quantique, Resonateur de grand facteur de Qualit  , Interf rom tres pour la detection d'ondes gravitationnelles, Bruit de pression de radiation quantique

Subject : Optomechanics and squeezed light

Abstract:

Keywords : Optomechanics, Squeezing, High-Finesse cavity, Interferometry, Thermal Noise, Quantum Shot Noise, High-Q Resonator, Gravitational wave Interferometer, Quantum Radiation Pressure Noise